Beyond the Born-Oppenheimer static surface model for molecule-surface reactions

Spiering, P.

Chapter 2

Theory

This chapter details the theoretical background neccesary to describe the interactions between molecules and metal surfaces needed for performing dynamical simulations, which can be directly compared with molecular beam experiments. In the scope of this thesis, the focus is on homonuclear diatomic molecules. In order to simplify the presentation, atomic units are used throughout this chapter ($\hbar = m_e = 1$).

2.1 Simulations of Molecular Beam Experiments

In a molecular beam experiment, molecules can be prepared in a specific (subject to experimental challenges) vibrational, rotational and electronic quantum state $|\Psi(\mathbf{R},\mathbf{r},t)_0\rangle$ in the gas phase. Obviously, the molecules are prepared in such a way that they are on a trajectory to collide with a surface. In principle, the time dependent Schrödinger equation can be used to model the time evolution of this experiment given the initial condition $|\Psi(\mathbf{R},\mathbf{r},t)_0\rangle$ according to

$$i\hbar\frac{\partial}{\partial t}|\Psi(\mathbf{R},\mathbf{r},t)\rangle = \hat{H}|\Psi(\mathbf{R},\mathbf{r},t)\rangle, \tag{2.1}$$

where $|\Psi(\mathbf{R},\mathbf{r},t)\rangle$ is the wave function of the system with nuclei $\mathbf{R}$ and electrons $\mathbf{r}$. The Hamiltonian ($\hat{H}$) describes all the relevant interactions between individual molecules in the surface.

In practice, Eq. 2.1 cannot be evaluated without further approximations in the context of molecular beam simulations, due to the large amount of computational effort required. In particular, it is often assumed that the quantum state $|\Psi(\mathbf{R},\mathbf{r},t)\rangle$ can be written as a product of the electronic (φ) and nuclear (ϕ) states together with the electronic ($\hat{H}_e$) and nuclear ($\hat{H}_N$) Hamiltonian according to

$$\hat{H}|\Psi(\mathbf{R},\mathbf{r},t)\rangle \approx \left(\hat{H}_N + \hat{H}_e\right)|\phi\rangle|\varphi\rangle, \tag{2.2}$$

within the Born-Oppenheimer approximation (BOA). The electronic system can then be solved first and separately by taking the electronic Hamiltonian

$$\hat{H}_e = \underbrace{\sum_{n=1}^{N_e}\frac{-\nabla^2_{\mathbf{r}_n}}{2}}_{\hat{T}_e} + \underbrace{\frac{1}{2}\sum_{m\neq n}^{N_e}\frac{1}{|\mathbf{r}_m-\mathbf{r}_n|}}_{\hat{V}_{ee}} - \underbrace{\sum_{n=1}^{N_e}\sum_{N=1}^{N_N}\frac{Z_N}{|\mathbf{R}_N-\mathbf{r}_n|}}_{\hat{V}_{Ne}} \tag{2.3}$$

where $\hat{T}_e$ is the kinetic energy of the electrons $\hat{T}_e$, the electron-electron interaction $\hat{V}_{ee}$ and the nuclear-electron interaction $\hat{V}_{Ne}$. The Schrödinger equation for the electronic system is then solved at a specific, i.e. depending parametrically on, nuclear configuration $\mathbf{R}$ according to

$$\hat{H}_e|\varphi(\mathbf{r},\mathbf{R})\rangle = V_e(R)|\varphi(\mathbf{r},\mathbf{R})\rangle, \tag{2.4}$$

where the eigenvalue $V_e(\mathbf{R})$ can then be interpreted as the energy of the electronic subsystem given the nuclear coordinates $\mathbf{R}$. Within the scope of this work Eq. 2.4 is used to solve for the electronic ground-state.

It is then possible to solve Eq. 2.2 for the nuclear system according to

$$\left(\hat{H}_N + \hat{V}_e\right)|\phi\rangle = V(R)\,|\phi\rangle\,, \tag{2.5}$$

since within the BOA the nuclear dynamics are completely defined by the ground state potential energy surface $V_e + V_{NN}$. The BOA is often justified because the coupling between the electronic and nuclear system, which is neglected here, has a magnitude of the ratio of the electron and nuclear masses, which is smaller than 10^{-3}. For molecules interacting with metal surfaces, this approximation is severely challenged: while the coupling for each state i is small due to the mass ratio, there is a large amount of states available for coupling at zero energetic cost due to the lack of a band gap. In fact, there are several (molecular and atomic beam) experiments that demonstrate the failure of the BOA [1, 2].

The following sections will describe how the potential energy is obtained and how the nuclear dynamics are calculated in this work. The potential energy (Sec. 2.2) is found by approximating the ground state electronic Hamiltonian using DFT and obtaining the concomitant ground-state energies. Nuclear dynamics as described by Eq. 2.5 are solved approximately using the method of quasi-classical (QC) dynamics (Sec. 2.3). Finally, the foundations of electronic friction theory are presented in Sec. 2.4, which allows to reintroduce effects beyond the BOA in a computationally affordable manner for molecules moving near metal surfaces. Based on these methods, observables have been computed that are accessible in molecular beam experiments. These results either stand as predictions, or can be compared with existing experimental data as a means of validating the underlying theoretical methodology and approximations.

2.2 Potential Energy

Given the computational demand for performing electronic structure calculations of even small molecules interacting with *metal* surfaces and the large amount of such

calculations needed for dynamics calculations, density functional theory (DFT) is currently the best compromise between accuracy and computational cost for the treatment of the electronic structure.

2.2.1 Density Functional Theory

The first Hohenberg-Kohn theorem states that there is a one-to-one mapping between the electronic wave function (φ), the electron density (ρ) and the so-called external potential (V_{ext}) which includes all external influences on the electronic system [3]. In the context of this work the external potential is given by the nuclear-electron interaction $\hat{V}_{Ne}$ (Eq. 2.3) since no other fields that may perturb the electronic system (e.g. external electric or magnetic fields) are considered.

Since the total energy (E) of the system can be defined by the functional $E[\varphi]$, it can also be defined by ρ or V_{ext} using

$$E[\varphi] \Leftrightarrow E[\rho] \Leftrightarrow E[V_{ext}]. \tag{2.6}$$

The functional defining the energy using ρ can be written as a sum of two contributions: the interaction of the electron density with the external potential ($V_{ext}[\rho]$) and the Hohenberg-Kohn functional ($F_{HK}[\rho]$) describing all other interactions according to

$$E[\rho] = V_{ext}[\rho] + F_{HK}[\rho]. \tag{2.7}$$

In the second Hohenberg-Kohn theorem, also known as the Hohenberg-Kohn variational principle, the ground state electron density ρ_0 is proven to minimize the total energy functional

$$E_0 := E[\rho_0] \leq E[\rho], \forall \rho \neq \rho_0. \tag{2.8}$$

The ground state can therefore be found by finding the stationary point using a functional derivative

$$\frac{\delta E[\rho]}{\delta \rho} = 0 \Rightarrow \rho_0. \tag{2.9}$$

Consequently, the ground state energy becomes a function of the nuclear coordinates according to

$$E_0[V_{ext}(\mathbf{R})] = E_0(\mathbf{R}), \tag{2.10}$$

which is exactly the definition of the PES needed to perform dynamics.

Unfortunately, the Hohenberg-Kohn functional is not known. In order to construct a (first) approximation, Kohn and Sham [4] have split up the Hohenberg-Kohn functional into the electrostatic interaction of the electron density with itself and the kinetic energy of the electron density.

$$E[\rho] = V_{ext}[\rho] + F_{HK}[\rho] = \underbrace{V_{ext}[\rho] + J[\rho] + T_s[\rho]}_{\text{exact}} + V_{xc}[\rho]. \tag{2.11}$$

The electrostatic interaction is approximated by the classical coulomb interactions of the electron density

$$J[\rho] = \frac{1}{2} \int d\mathbf{r} d\mathbf{r}' \frac{\rho(\mathbf{r})\rho(\mathbf{r}')}{|\mathbf{r} - \mathbf{r}'|}. \tag{2.12}$$

In order to evaluate the kinetic energy, Kohn and Sham have reintroduced orbitals, denoted here as Kohn-Sham orbitals φ_i^{KS}, that represent a fictitious system of n non-interacting electrons with the same density as a system of interacting electrons. The density is given in terms of the Kohn-Sham orbitals as

$$\rho\left(\left\{\varphi_1^{\mathsf{KS}}..\varphi_n^{\mathsf{KS}}\right\}\right) = \sum_i \langle \varphi_i^{\mathsf{KS}} | \varphi_i^{\mathsf{KS}} \rangle . \tag{2.13}$$

The kinetic energy is then approximated by a quantum system with the same electron density, but where the electrons do not interact

$$T_s[\rho] = \sum_i \langle \varphi_i^{\mathsf{KS}} | \frac{-\nabla^2}{2} | \varphi_i^{\mathsf{KS}} \rangle . \tag{2.14}$$

A certain part of the electron-electron interaction is not correctly described by $J[\rho]$ and, likewise, $T_s[\rho]$ does not correctly describe the energy for interacting electrons. These contributions are collected in the exchange-correlation functional $V_{xc}[\rho]$, for which approximations are discussed below.

The Kohn-Sham equations are effective single particle Schrödinger equations that result from reexpressing the total density constrained Hohenberg-Kohn variational principle

$$\frac{\delta}{\delta\rho}\left(E\left[\rho\right] - \mu\left(\int d\mathbf{r}\rho(\mathbf{r}) - n\right)\right) = 0, \tag{2.15}$$

with Lagrangian multiplier μ, in terms of the Kohn-Sham orbitals according to

$$\left(\frac{-\nabla^2}{2} + v_{eff}\right)\varphi_i^{\mathsf{KS}} = \epsilon_i \varphi_i^{\mathsf{KS}}. \tag{2.16}$$

Here v_{eff} is given by

$$v_{eff}(\mathbf{r}) = \underbrace{\int d\mathbf{r}' \frac{\rho(\mathbf{r}')}{|\mathbf{r}-\mathbf{r}'|}}_{v_{\mathsf{Coul}}} + \underbrace{\frac{\delta V_{Ne}[\rho]}{\delta\rho(\mathbf{r})}}_{v_{\mathsf{ext}}} + \underbrace{\frac{\delta V_{xc}[\rho]}{\delta\rho(\mathbf{r})}}_{v_{\mathsf{XC}}}, \tag{2.17}$$

with v_{ext} being the one-electron external potential. Solving Eqs. 2.11 and 2.16 self-consistently from an initial guess of the Kohn-Sham orbitals then yields the single particle energies ϵ_i and the total energy is given by

$$E[\rho] = \sum_i \epsilon_i - J[\rho] + V_{xc}[\rho] - \int d\mathbf{r} v_{xc}[\rho](\mathbf{r}). \tag{2.18}$$

There are several classes of approximations for the exchange-correlation functionals. In the local density approximation (LDA) the exchange-correlation functional is designed to reproduce the homogeneous electron gas (HEG)

$$V[\rho] = \int d\mathbf{r}\rho(\mathbf{r}) v_{xc}^{\mathrm{HEG}}(\rho(\mathbf{r})), \tag{2.19}$$

and is based on local evaluations of the density only. The generalised gradient approximation (GGA) the gradient of the electron density is also evaluated as a first order approximation to non-local effects,

$$V[\rho] = \int d\mathbf{r}\rho(\mathbf{r}) v_{xc}^{\mathrm{GGA}}(\rho(\mathbf{r}), \nabla_{\mathbf{r}}\rho(\mathbf{r})), \tag{2.20}$$

which for most applications is an improvement compared to the LDA. A further improvement to the accuracy is the meta-GGA which includes even more non-local effects. Including the higher order non-local contributions generally comes at an increased computational effort.

In this thesis functionals at the GGA level (mainly PBE [5, 6] and RPBE [7], depending on the system) constitute the main 'work horses' for the construction of PESs. In addition, the semi-empirically motivated SRP method [8] is used where a

new functional is created by taking the linear combination of two existing functionals A and B based on the parameter α

$$E[\rho] = V_{ext}[\rho] + J[\rho] + T_s[\rho] + \alpha V_{xc}^{\mathrm{A}}[\rho] + (1-\alpha)V_{xc}^{\mathrm{B}}[\rho], \tag{2.21}$$

in such a way that an experimental observable is reproduced more accurately. Ideally, the (groundstate) PES given by this new functional is better approximated than by the underlying functionals.

2.2.2 Continuous Representations of the Potential Energy Surface

While DFT is in principle able to produce $V_e(\mathbf{R})$ needed to solve the nuclear Schrödinger equation 2.5, it is neccesary to obtain this potential for all configurations $\mathbf{R}$ of the nuclear system that are relevant for the dynamics in a simulation of a molecular beam experiment. One way to do this is to do *ab-initio* molecular dynamics (AIMD) by performing a DFT calculation every time $V_e(\mathbf{R})$ is needed for a specific configuration $\mathbf{R}$ during the dynamics. However, if one is interested in obtaining observables with statistical significance for rare events during dynamics, such as reactions for molecules with a very low reaction probability, this becomes too computationally demanding. Instead, continuous representations of the PES are used. Generally, a large data set of configurations with concomitant energies is generated which is consequently interpolated or fitted. When the resulting continuous representation is not of sufficient quality, a larger data set can be obtained, or a different strategy can be used. For diatomic molecules, the coordinates $\mathbf{R}$ can be conveniently described w.r.t. a surface atom in the first layer as two single atom Cartesian coordinates $\mathbf{R}_A$ and $\mathbf{R}_B$, or using the molecular coordinate system where the center of mass (COM) (equivalent to the geometric centre for homonuclear molecules) X, Y and Z coordinates are used together with the bond distance r, polar angle θ, and azimuthal angle ϕ (see Fig. 2.1). Three different methods have been used in this thesis to obtain continuous representations of PESs. First the corrugation reducing procedure (CRP) in combination with an interpolation using symmetry adapted basis functions is used for H_2 interacting with (an ideal 0K) Cu(111) surface (Chap. 3). This method only allows for 6 degrees of freedom of the

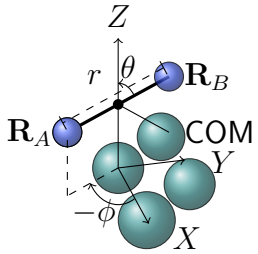

Figure 2.1: Six-dimensional coordinate system for the description of diatomic molecules (atoms in blue) on metal surfaces (atoms in green), consisting of the center of mass (COM) coordinates (X,Y,Z) and the bond distance r as well as the polar angle θ and azimuthal angle ϕ. X,Y,Z = 0 corresponds to the position of a surface layer atom in the surface plane (top site).

molecule while the motion and displacements of the metal is neglected. Secondly, the SCM model (Chap. 3) allows to introduce the effect of surface atom displacements. This effect is introduced within a so-called sudden approximation and realised as a perturbation to the 6D CRP PES. Such a treatment precludes energy exchange with the phonons of the surface. Finally, to also include the effect of surface motion, NN fits (Chap. 5) have been used to model all degrees of freedom of the nuclear system.

Corrugation Reducing Procedure

Within the CRP, the PES is represented by

$$V_{CRP}(\mathbf{R}) = V_{3D}(\mathbf{R}_A) + V_{3D}(\mathbf{R}_B) + I_{6D}(\mathbf{R}), \tag{2.22}$$

as sum of two 3D potentials (V_{3D}), which describe the interaction of two independent atoms A and B with the metal surface, and a 6D interpolation function (I_{6D}), which describes the molecular contribution of the system. Here $\mathbf{R} = (\mathbf{R}_A, \mathbf{R}_B)$ represents the coordinate vector composed of both individual atom coordinate vectors $\mathbf{R}_A$ and $\mathbf{R}_B$. Much of the corrugation is then already contained in the 3D potentials and the rest

term is then more easily interpolated. The 3D potential

$$V_{3D}(\mathbf{R}_x) = \sum_i^N V_{1D,ref}(|\mathbf{R}_x - \mathbf{S}_i|) + I_{3D}(\mathbf{R}_x), x \in \{A, B\} \tag{2.23}$$

consists of the sum of two-body interactions ($V_{1D,ref}$) with the N closest surface atoms, described by the vectors $\mathbf{S}_i$ together with a 3D interpolation function (I_{3D}). Surface symmetry (C_{3v}) and periodicity can be fully taken into account using the CRP. The 3D and 6D interpolation functions are based on symmetry adapted basis functions defined using the Grand Orthogonality Theorem. For the 6D interpolation function a spline interpolation is made for several 2D PES cuts in the r-Z plane at several surface sites (X,Y) and molecular orientations (ϕ,θ). The symmetry adapted basis functions are then used to interpolate between the different r-Z cuts. Because the error of the CRP interpolation is generally much smaller than that of the underlying DFT, it is considered appropriate to use the CRP to represent the 6D PES.

Static Corrugation Model

The effect of surface atom displacements can be taken into account by treating the displacements as perturbations to the ideal lattice using the SCM, which has originally been developed by Wijzenbroek and Somers [9] Chap. 3 describes the model in detail, together with the further development and improvments that are introduced as part of this thesis [10].

Neural Networks

For the reactive scattering of N_2 on Ru(0001) a significant amount of energy exchange with the phonons of the surface has been found. Consequently, a significant influence of surface motion on the dissociative chemisorption probability was also observed [11, 12]. Thus both the CRP and SCM are not suitable for this system. Instead a continuous representation of the PES including surface atom motion has been obtained using a high-dimensional NN [12]. In order for the NN to predict energies with the correct symmetry, the Behler-Parrinello method has been used [13, 14]. This method uses radial and angular symmetry functions to describe the chemical environment for each

atom in the system. The total PES is decomposed into individual atomic contributions, where differently optimized NN-parameters are used for different atom types. The resulting single atom energies are added together, ensuring the correct symmetry. In Chap. 6 more details on NN topologies are provided. Although the focus there is not on PESs, this details also apply for NN-based PES representation.

2.3 Quasi-Classical Molecular Dynamics

Using any of the previously discussed continuous PES representations(CRP plus SCM or NN), it is possible to describe the dissociative chemisorption and rovibrational (in)elastic scattering of diatomic molecules on metal surfaces. The PES itself is not a directly measurable quantity, but it is possible to do molecular dynamics simulations with the PES to compute observables. In this thesis, dynamics simulations were performed of H_2 and N_2 molecules coming from the gas phase towards a Cu(111) and Ru(0001) surface respectively, in a collision event. The dynamics were performed using the method of QC dynamics [8, 11, 15].

A dynamics calculation is performed by first determining the initial configuration for the molecule and in the case of a non-zero surface temperature also determining the initial displacements of surface atoms from their equilibrium positions. Initial conditions are determined using a Monte-Carlo sampling scheme, where zero point energy is taken into account for the initial configuration of the molecule. Then the system is propagated classically by solving Newton's equations of motion until certain stopping criteria are fulfilled and the resulting trajectory is then analysed. This process is repeated many (10^4 to 10^6) times - depending on the observable to be calculated - to get a good statistical average using the Monte-Carlo scheme. The details are discussed in the following sections.

2.3.1 Initial Conditions

The initial conditions are generated by first calculating the rovibrational energy levels of the diatomic molecule for their respective PES in the gas phase using the Fourier grid

Hamiltonian method [16]. To get the QC distribution for the atom-atom separation r of the molecule, the gasphase molecule was propagated for one complete phase in its vibration, after which the initial atomic positions and velocities were chosen using standard Monte Carlo methods such that the sampling is homogenous in time. The ϕ angle is chosen from an uniform random distribution in the range $[0, 2\pi]$ while θ is chosen from an uniform random distribution in the range $[0, \theta_L]$ where $\theta_L = \pi$ if J=0 and $cos(\theta_L) = \frac{m_J}{\sqrt{J(J+1)}}$ if J≥1. The angular velocities are chosen according to the quantized angular momentum $L^2 = J(J+1)\hbar^2$. The initial COM position is then shifted 9 Å in Z away from the surface (Z=9 Å) while the COM position along the surface is given by X = U + $\frac{1}{2}$V and Y = $\frac{1}{2}\sqrt{3}$V where U and V are chosen from an uniform random distribution in the range $[0, a]$ with a being the lattice constant. This process is identical to earlier work [8, 9, 15, 17, 18]. In the case of finite surface temperature, a detailed description of the surface atom displacement is given in Chap. 3.

2.3.2 Propagation

Once the initial conditions are defined, the system is propagated according to Hamilton's formulation of classical mechanics, i.e. based on the Hamiltionian

$$H = \frac{p_A^2(t)}{2m_A} + \frac{p_B^2(t)}{2m_B} + V(R(t)), \tag{2.24}$$

where $p_A(t)$ and $p_B(t)$ are the momenta of atoms A and B respectively at time t and $V(R(t))$ is the potential energy at time t. The time propagation of simulations of H_2 have been performed using the predictor-corrector method of Bulirsch and Stoer [19]. Simulations with N_2 on the other hand have been propagated as detailed in Sec. 2.4. The propagation of a trajectory is stopped when either the maximum time limit has been reached (as detailed in the respective chapters), or the H (N) atoms are separated by more than 2.25Å (2.75Å), in which case the original corresponding diatomic is considered to have dissociated (i.e. reacted).

2.3.3 Analysis

After a trajectory has been stopped, it is analysed to determine the outcome.

Reaction Probability

The reaction probability is defined as the number of trajectories that result in a reaction, divided by the total number of trajectories and gives a measure of how likely it is for the reaction to take place under a certain set of initial conditions (e.g. molecular velocity distribution and/or rovibrational state, surface temperature).

Rovibrational Elastic and Inelastic Scattering

When an incoming trajectory is not reactive, it can either scatter back into the gasphase or get trapped on the surface. The incoming trajectories that turn out to scatter can be divided into two groups: either the molecule returns from the surface in the same rovibrational state, or it does not. Scattered molecules in the same rovibrational state are considered to have scattered elastically, while scattered molecules that are not in the same rovibrational state are considered to have scattered inelastically. In order to relate the outcome of a quasiclassical trajectory to a (discrete) rovibrational quantum state a binning procedure is necessary. That means that the final rovibrational energy has to be assigned to a rotational (J) and a vibrational (v) state. Generally the energy difference between rotational states is much smaller than vibrational states which means if the total rovibrational energy of two states is similar, we can easily distinguish by first binning to the rotational state and then to the vibrational state. The quantum rotational state J has a direct classical analogue according to

$$L^2 = J(J+1). \tag{2.25}$$

The rotational state of a molecule in the quasiclassical approximation can be described in a similar way as a quantum rotational state by first assigning a non-integer number for J. Next the value of J is rounded while taking into account selection rules. These selection rules preclude a transition of J before the collision with the surface to a J after the collision that is different by an odd number. This approach works because

L is well defined in classical dynamics. For a classical trajectory, the momenta of all atoms are known at all times. If there is no interaction between the surface and the diatomic molecule at the time of analysis, i.e. at sufficiently large molecular-surface distances, the angular momentum L of the diatomic is conserved and given by

$$L = |\overrightarrow{r} \times \overrightarrow{p}|\,, \tag{2.26}$$

where $\overrightarrow{r}$ is the distance vector from one atom to the other and $\overrightarrow{p} = \mu\dot{\overrightarrow{r}}$ is the momentum vector along the internal coordinates of the molecule with

$$\mu = \frac{m_A m_B}{m_A + m_B}. \tag{2.27}$$

When the J state is assigned, the rovibrational energy of the scattered molecule (E_{rovib}) is determined by subtracting the COM kinetic energy ($E_{kin,COM}$) and the potential energy ($V(r)$) relative to the equilibrium potential energy ($V(r_0)$) from the total kinetic energy of the molecule according to

$$E_{rovib} = E_{kin} - E_{kin,COM} - (V(r_0) - V(r))\,. \tag{2.28}$$

The COM kinetic energy for a diatomic is defined by

$$E_{kin,COM} = \frac{(m_A + m_B)\left(\dot{X}^2 + \dot{Y}^2 + \dot{Z}^2\right)}{2}. \tag{2.29}$$

The rovibrational energy is then compared to the rovibrational eigenstates of the molecule that has the previously determined J state (according to Eqs. 2.25 and 2.26) and the candidate with the closest energy is selected.

2.4 Nuclear Dynamics Beyond the Born-Oppenheimer Approximation

With dynamics on a (single) PES, it is not possible to take into account the exchange of energy between the electronic and nuclear system due to electron-nuclear couplings that are neglected within the BOA. In order to reintroduce the effect of these couplings and

concomitant electron-hole pair excitations on the nuclear dynamics (while maintaining a classical description of the latter), electronic friction theory [20, 21] is used in this work. This work-horse theory for dynamics of molecules on metal surfaces, which can be considered as "weakly non-adiabatic", is based on a generalized Langevin equation (GLE)

$$m_i \frac{d^2 \{\mathbf{R}, \mathbf{S}\}_i}{dt} = -\nabla_i V(\mathbf{R}, \mathbf{S}) \; - \underbrace{\sum_j \eta_{ij}^{\mathsf{mol}}(\mathbf{R}) \frac{dR_j}{dt}}_{\text{dissipative}} + \underbrace{\mathcal{F}^{\mathsf{mol}}(\boldsymbol{\eta}, T_\mathrm{s})}_{\text{random}} \quad . \tag{2.30}$$

This equation introduces two additional terms compared to Newtonian dynamics (see previous section): a dissipative term based on the electronic friction tensor η^{mol} and the velocities $\frac{d\mathbf{R}}{dt}$, and random forces $\mathcal{F}^{\mathsf{mol}}$ that depend on the surface temperature T_s and the friction tensor. The friction tensor is based on matrix elements that couple the electronic and nuclear system and the GLE thus goes beyond the Born-Oppenheimer Approximation. Motivated by previous work [22–25], in this thesis the focus has been on obtaining electronic friction coefficients for the diatomic molecule $\mathbf{R}$ but not for the surface atoms $\mathbf{S}$.

The non-adiabatic energy loss, i.e. energy that is dissipated into electron-hole pairs at time t starting from time t_0, in the absence of random forces, is given by

$$E_{\mathsf{diss}}(t) = \int_{t'=t_0}^{t} dt' \dot{R}_i(t') \eta_{ij}(\mathbf{R}(t')) \dot{R}_j(t'). \tag{2.31}$$

All dynamical calculations for H_2 on Cu(111) including electronic friction make use of the static surface approximation ($T_s = 0$ K), for which the stochastic term ($\mathcal{F}^{\mathsf{mol}}$) vanishes (see also Chap. 4). The calculations for N_2 on Ru(0001) on the other hand have been performed for a surface temperature $T_S = 575$ K. In order to do so, the "OVRVO" algorithm of Sivak, Chodera, and Crooks [26] has been adapted (see Chap. 5). This algorithm is a split-operator method where first half a time step of friction and random force is propagated using the Ornstein–Uhlenbeck (O) method [27], then half a time step of the deterministic velocity (V) is updated, next a full time step of the deterministic position (R) is updated and finally half a time step of V and then O are updated. When no friction is present, this algorithm simplifies to the velocity-Verlet algorithm.

Already in 1975 have Suhl and coworkers [20] derived an expression for the electronic friction tensor (here expressed for spin-unpolarized systems)

$$\eta_{ij}^{\mathsf{mol}} = 2\pi \sum_{m,n} \langle \psi_m | \hat{F}_i | \psi_n \rangle \langle \psi_n | \hat{F}_j | \psi_m \rangle \times \delta(\epsilon_{\mathsf{F}} - \epsilon_m)\, \delta(\epsilon_{\mathsf{F}} - \epsilon_n)\,. \tag{2.32}$$

Their derivation is based on a "bootstrap" method to compare the friction tensor $\boldsymbol{\eta}^{\mathsf{fric}}$ based on the Fokker-Planck equation with rigorous formulas using the full Hamiltonian of the system. Here $\hat{F}_{i,j}$ describes the response of a perturbation to the electronic system of the adsorbate-surface system within a single-particle picture with states ψ_n,ψ_m and concomitant energies ϵ_n,ϵ_m. The perturbation results from the motion along adsorbate coordinates R_i and R_j in the limit of slow adsorbate motion (quasi-static limit) and small electronic temperatures corresponding to energy equivalents that are small relative to the Fermi energy ϵ_{F} of the metal.

Subotnik and coworkers [28–31] have shown that there is only one "universal" electronic friction tensor, which is the temperature dependent version of Eq. 2.32. Other formulations of electronic friction then are either equivalent or contain further approximations.

In this thesis I have used two methods to calculate electronic friction coefficients (i.e. elements of the friction tensor): i) the Local-Density Friction Approximation (LDFA) [25, 32] where the friction tensor of an atom in jelium is computed and ii) the orbital-dependent friction (ODF) [20, 21, 33–36] where the friction tensor is obtaind from density functional perturbation theory (density functional perturbation theory (DFPT)). Detailed derivations of both LDFA and ODF can be found elsewhere [20, 28, 29]. Brief summaries of these derivations are presented in the remainder of this section since some of the underlying approximations are important for comparing the LDFA and ODF results as is done later in this thesis.

2.4.1 Local Density Friction Approximation

Within the LDFA Eq. 2.32 is used to evaluate the electronic friction tensor of a model system, namely an atom (moving) in a homogeneous electron gas (jellium) with a given density ρ_e. In this case the matrix elements $\langle \psi_m | \hat{F}_i | \psi_n \rangle$ can be conveniently

obtained by considering the scattering of the electronic continuum from the nucleus of the atom embedded therein. Assuming spherical symmetry, the scattering problem becomes (effectively) one dimensional, and the aforementioned matrix elements can be obtained from the scattering phase shifts of partial (spherical) waves belonging to different angular momentum channels l. As a result of the spherical Hamiltonian assumption, the friction tensor becomes diagonal in Cartesian coordinates and the elements are the same in every direction for the same atom and jelium, resulting in a single friction coefficient per atom.

$$\eta^{\mathsf{AiJ}}\left(\rho_e\right) = \rho_e \frac{8}{3\pi}\epsilon_{\mathsf{F}} \sum_l \left(l+1\right)\sin^2\left(\delta_l - \delta_{l+1}\right). \tag{2.33}$$

Juaristi and coworkers [24] have suggested to use these friction coefficients for simulations of molecular beam experiments on metal surfaces. Diatomic molecules are treated within an independent atom approximation. That means that the friction coefficient for each individual atom is taken as the friction of that atom in a jelium with an electron density ρ_e equal to that of the electron density of a clean metal surface, at the position of the atom $\mathbf{R}_A$:

$$\eta^{\mathsf{LDFA}}\left(\mathbf{R}_A\right) = \eta^{\mathsf{AiJ}}\left(\rho_e^{\mathsf{clean\ surface}}\left(\mathbf{R}_A\right)\right). \tag{2.34}$$

The friction coefficient for a specific atom is then computed for several electron densities and a simple analytical fit is made to map the density to the friction coefficient. These friction coefficients can easily be fitted in 3D, e.g. by using machine learning techniques (NNs).

2.4.2 Orbital-Dependent Friction

Within a Kohn-Sham (KS) time-dependent DFT picture, an expression corresponding to Eq. 2.32 for the electronic friction tnesor has been obtained by various authors [21, 33, 35, 37, 38]. Unlike for LDFA, the matrix elements of this "orbital-dependent" friction (ODF) tensor are based on the KS orbitals of atoms and molecules on an actual metal surface and the changes of the KS effective potential due to motion

$$\eta_{ij}^{\mathsf{ODF}} = 2\pi \sum_{m,n} \langle\psi_m^{\mathsf{KS}}| \frac{\partial v_{\mathsf{eff}}^{\mathsf{KS}}}{\partial R_i} |\psi_n^{\mathsf{KS}}\rangle \langle\psi_n^{\mathsf{KS}}| \frac{\partial v_{\mathsf{eff}}^{\mathsf{KS}}}{\partial R_j}^* |\psi_m^{\mathsf{KS}}\rangle \, \delta\left(\epsilon_n^{\mathsf{KS}} - \epsilon_{\mathsf{F}}\right) \delta\left(\epsilon_m^{\mathsf{KS}} - \epsilon_{\mathsf{F}}\right). \tag{2.35}$$

These so-called electron-phonon matrix elements $\langle\psi_n^{\mathsf{KS}}|\,\frac{\partial v_{\mathsf{eff}}^{\mathsf{KS}}}{\partial R_i}\,|\psi_m^{\mathsf{KS}}\rangle$ can be conveniently obtained from DFPT. Within DFPT, the Kohn-Sham equations are rewritten in a derivative form, where a change in the position of nuclear coordinates is considered. The Kohn-Sham equations now become

$$\left(\frac{-\nabla^2}{2}+v_{\mathsf{eff}}^{\mathsf{KS}}-\epsilon_m^{\mathsf{KS}}\right)|\Delta_i\varphi_m^{\mathsf{KS}}\rangle=-\left(\Delta_i v_{\mathsf{eff}}^{\mathsf{KS}}-\Delta_i\epsilon_m^{\mathsf{KS}}\right)|\varphi_m^{\mathsf{KS}}\rangle\,, \tag{2.36}$$

where $\Delta_i=\frac{\partial}{\partial R_i}$ denotes the potential derivative with respect to nuclear displacement R_i. Eq. 2.36 leaves some room for interpretation on how to sum over the states n and m, especially when considering a periodic system where also a k-point index is introduced. Throughout this thesis, the method of Trail, Graham, and Bird [39] for an overlayer of adsorbates on a metal surface is used when performing this summation. Both the perturbation of the external potential $\Delta_i v_{\mathsf{ext}}$ and an induced perturbation due to the response of the system are included in the change of the effective potential according to

$$\Delta_i v_{\mathsf{eff}}^{\mathsf{KS}}=\underbrace{\Delta_i v_{\mathsf{ext}}}_{\text{perturbation}}+\underbrace{\int d\mathbf{r}'\frac{\Delta_i\rho\,(\mathbf{r}')}{|\mathbf{r}-\mathbf{r}'|}+\left.\frac{\delta v_{\mathsf{XC}}\,(\rho)}{\delta\rho}\right|_{\rho=\rho(\mathbf{r})}\Delta\rho\,(\mathbf{r})}_{\text{induced}}\,. \tag{2.37}$$

The perturbed quantities $\Delta_i\epsilon_m^{\mathsf{KS}}$, $\Delta_i\varphi_m^{\mathsf{KS}}$ and $\Delta_i\rho$ are found by

$$\Delta_i\epsilon_m^{\mathsf{KS}}=\langle\varphi_m^{\mathsf{KS}}|\,\Delta_i v_{\mathsf{eff}}^{\mathsf{KS}}\,|\varphi_m^{\mathsf{KS}}\rangle\,, \tag{2.38}$$

$$\Delta_i\varphi_m^{\mathsf{KS}}=\sum_{n\neq m}\varphi_n^{\mathsf{KS}}\frac{\langle\varphi_n^{\mathsf{KS}}|\,\Delta_i v_{\mathsf{eff}}^{\mathsf{KS}}\,|\varphi_m^{\mathsf{KS}}\rangle}{\epsilon_m^{\mathsf{KS}}-\epsilon_n^{\mathsf{KS}}}, \tag{2.39}$$

and

$$\Delta_i\rho=4\sum_{m=1}^{N/2}\sum_{n\neq m}\varphi_m^{\mathsf{KS}*}\varphi_n^{\mathsf{KS}}\frac{\langle\varphi_n^{\mathsf{KS}}|\,\Delta_i v_{\mathsf{eff}}^{\mathsf{KS}}\,|\varphi_m^{\mathsf{KS}}\rangle}{\epsilon_m^{\mathsf{KS}}-\epsilon_n^{\mathsf{KS}}} \tag{2.40}$$

respectively. Solving Eqs. 2.36 through 2.40 self-consistently (as nowadays implemented in many standard DFT packages) yields the neccesary electron-phonon matrix elements.

From a computational point of view, it is important to note that the δ-functions in the 'sum over states' (Eq. 2.35) cannot be analytically eliminated - unlike in the (final) expression for for η^{LDFA} (Eq. 2.33). For a summation over a finite set of states, which

are not all located at the Fermi surface (for practical reasons), the δ-functions thus are broadened, i.e., usually substituted by Gaussians with a finite width [34–36, 40–44]. This approximation has been criticized by Novko and coworkers [45] and might in the future be overcome by a new technique, which has been suggested only very recently by Jin and Subotnik [46].

A continuous representation of η_{ij}^{ODF} that accounts for symmetries of the adsorbate-surface system is by far not as easy to obtain as $\eta_{ij}^{\mathsf{LDFA}}$. The representations used in Chap. 4 and Chap. 5 have been developed as part of this thesis, and the underlying methodology is described in detail in Chap. 6.

References

[1] A. M. Wodtke. “Electronically Non-Adiabatic Influences in Surface Chemistry and Dynamics”. In: *Chem. Soc. Rev.* 45 (2016), pp. 3641–3657. DOI: 10.1039/C6CS00078A.

[2] A. M. Wodtke, J. C. Tully, and D. J. Auerbach. “Electronically Non-Adiabatic Interactions of Molecules at Metal Surfaces: Can We Trust the Born-Oppenheimer Approximation for Surface Chemistry?” In: *Int. Rev. Phys. Chem.* 23.4 (2004), pp. 513–539.

[3] P. Hohenberg and W. Kohn. “Inhomogeneous Electron Gas”. In: *Phys. Rev.* 136 (1964), B864–B871. DOI: 10.1103/PhysRev.136.B864.

[4] W. Kohn and L. J. Sham. “Self-Consistent Equations Including Exchange and Correlation Effects”. In: *Phys. Rev.* 140 (1965), A1133–A1138. DOI: 10.1103/PhysRev.140.A1133.

[5] J. P. Perdew, K. Burke, and Y. Wang. “Generalized Gradient Approximation for the Exchange-Correlation Hole of a Many-Electron System”. In: *Phys. Rev. B* 54 (1996), pp. 16533–16539. DOI: 10.1103/PhysRevB.54.16533.

[6] J. P. Perdew, K. Burke, and M. Ernzerhof. “Erratum: Generalized Gradient Approximation Made Simple [Phys. Rev. Lett. 77, 3865 (1996)]”. In: *Phys. Rev. Lett.* 78 (1997), pp. 1396–1396. DOI: 10.1103/PhysRevLett.78.1396.

[7] B. Hammer, L. B. Hansen, and J. K. Nørskov. “Improved Adsorption Energetics within Density-Functional Theory Using Revised Perdew-Burke-Ernzerhof Functionals”. In: *Phys. Rev. B* 59 (1999), pp. 7413–7421. DOI: 10.1103/PhysRevB.59.7413.

[8] C. Díaz, E. Pijper, R. A. Olsen, H. F. Busnengo, D. J. Auerbach, et al. "Chemically Accurate Simulation of a Prototypical Surface Reaction: H2 Dissociation on Cu(111)". In: *Science* 326 (2009), pp. 832–834. DOI: 10.1126/science.1178722.

[9] M. Wijzenbroek and M. F. Somers. "Static Surface Temperature Effects on the Dissociation of H2 and D2 on Cu(111)". In: *J. Chem. Phys.* 137 (2012), p. 054703. DOI: 10.1063/1.4738956.

[10] P. Spiering, M. Wijzenbroek, and M. F. Somers. "An Improved Static Corrugation Model". In: *J. Chem. Phys.* 149 (2018), p. 234702. DOI: 10.1063/1.5058271.

[11] K. Shakouri, J. Behler, J. Meyer, and G.-J. Kroes. "Analysis of Energy Dissipation Channels in a Benchmark System of Activated Dissociation: N2 on Ru(0001)". In: *J. Phys. Chem. C* 122 (2018), pp. 23470–23480. DOI: 10.1021/acs.jpcc.8b06729.

[12] K. Shakouri, J. Behler, J. Meyer, and G.-J. Kroes. "Accurate Neural Network Description of Surface Phonons in Reactive Gas–Surface Dynamics: N_2 + Ru(0001)". In: *J. Phys. Chem. Lett.* 8 (2017), pp. 2131–2136. DOI: 10.1021/acs.jpclett.7b00784.

[13] J. Behler, S. Lorenz, and K. Reuter. "Representing Molecule-Surface Interactions with Symmetry-Adapted Neural Networks". In: *J. Chem. Phys.* 127 (2007), p. 014705. DOI: 10.1063/1.2746232.

[14] J. Behler and M. Parrinello. "Generalized Neural-Network Representation of High-Dimensional Potential-Energy Surfaces". In: *Phys. Rev. Lett.* 98 (2007), p. 146401. DOI: 10.1103/PhysRevLett.98.146401.

[15] C. Diaz, R. A. Olsen, H. F. Busnengo, and G.-J. Kroes. "Dynamics on Six-Dimensional Potential Energy Surfaces for H2/Cu(111): Corrugation Reducing Procedure versus Modified Shepard Interpolation Method and PW91 versus RPBE". In: *J. Phys. Chem. C* 114 (2010), pp. 11192–11201. DOI: 10.1021/jp1027096.

[16] C. C. Marston and G. G. Balint-Kurti. "The Fourier Grid Hamiltonian Method for Bound State Eigenvalues and Eigenfunctions". In: *J. Chem. Phys.* 91 (1989), pp. 3571–3576. DOI: 10.1063/1.456888.

[17] A. Mondal, M. Wijzenbroek, M. Bonfanti, C. Díaz, and G.-J. Kroes. "Thermal Lattice Expansion Effect on Reactive Scattering of H2 from Cu(111) at Ts = 925 K". In: *J. Phys. Chem. A* 117 (2013), pp. 8770–8781. DOI: 10.1021/jp4042183.

[18] F. Nattino, A. Genova, M. Guijt, A. S. Muzas, C. Díaz, et al. "Dissociation and Recombination of D_2 on Cu(111): Ab Initio Molecular Dynamics Calculations and Improved Analysis of Desorption Experiments". In: *J. Chem. Phys.* 141 (2014), p. 124705. DOI: 10.1063/1.4896058.

[19] J. Stoer and R. Bulirsch. *Introduction to Numerical Analysis*. New York: Springer-Verlag, 1980.

[20] E. G. d'Agliano, P. Kumar, W. Schaich, and H. Suhl. "Brownian Motion Model of the Interactions between Chemical Species and Metallic Electrons: Bootstrap Derivation and Parameter Evaluation". In: *Phys. Rev. B* 11 (1975), pp. 2122–2143. DOI: 10.1103/PhysRevB.11.2122.

[21] M. Head-Gordon and J. C. Tully. "Molecular Dynamics with Electronic Frictions". In: *J Chem Phys* 103 (1995), pp. 10137–10145. DOI: 10.1063/1.469915.

[22] D. Novko, M. Blanco-Rey, M. Alducin, and J. I. Juaristi. "Surface Electron Density Models for Accurate *Ab Initio* Molecular Dynamics with Electronic Friction". In: *Phys. Rev. B* 93 (2016), p. 245435. DOI: 10.1103/PhysRevB.93.245435.

[23] A. C. Luntz, I. Makkonen, M. Persson, S. Holloway, D. M. Bird, et al. "Comment on "Role of Electron-Hole Pair Excitations in the Dissociative Adsorption of Diatomic Molecules on Metal Surfaces"". In: *Phys. Rev. Lett.* 102 (2009), p. 109601. DOI: 10.1103/PhysRevLett.102.109601.

[24] J. I. Juaristi, M. Alducin, R. D. Muiño, H. F. Busnengo, and A. Salin. "Juaristi et al. Reply:" in: *Phys. Rev. Lett.* 102 (2009), p. 109602. DOI: 10.1103/PhysRevLett.102.109602.

[25] J. I. Juaristi, M. Alducin, R. D. Muiño, H. F. Busnengo, and A. Salin. "Role of Electron-Hole Pair Excitations in the Dissociative Adsorption of Diatomic Molecules on Metal Surfaces". In: *Phys. Rev. Lett.* 100 (2008), p. 116102. DOI: 10.1103/PhysRevLett.100.116102.

[26] D. A. Sivak, J. D. Chodera, and G. E. Crooks. "Time Step Rescaling Recovers Continuous-Time Dynamical Properties for Discrete-Time Langevin Integration of Nonequilibrium Systems". In: *J. Phys. Chem. B* 118 (2014), pp. 6466–6474. DOI: 10.1021/jp411770f.

[27] G. E. Uhlenbeck and L. S. Ornstein. "On the Theory of the Brownian Motion". In: *Phys. Rev.* 36 (1930), pp. 823–841. DOI: 10.1103/PhysRev.36.823.

[28] W. Dou and J. E. Subotnik. "Perspective: How to Understand Electronic Friction". In: *J. Chem. Phys.* 148 (2018), p. 230901. DOI: 10.1063/1.5035412.

[29] W. Dou, G. Miao, and J. E. Subotnik. "Born-Oppenheimer Dynamics, Electronic Friction, and the Inclusion of Electron-Electron Interactions". In: *Phys. Rev. Lett.* 119 (2017), p. 046001. DOI: 10.1103/PhysRevLett.119.046001.

[30] W. Dou and J. E. Subotnik. "Universality of Electronic Friction: Equivalence of von Oppen's Nonequilibrium Green's Function Approach and the Head-Gordon–Tully Model at Equilibrium". In: *Phys. Rev. B* 96 (2017), p. 104305. DOI: 10.1103/PhysRevB.96.104305.

[31] W. Dou and J. E. Subotnik. "Universality of Electronic Friction. II. Equivalence of the Quantum-Classical Liouville Equation Approach with von Oppen's Nonequilibrium Green's Function Methods out of Equilibrium". In: *Phys. Rev. B* 97 (2018), p. 064303. DOI: 10.1103/PhysRevB.97.064303.

[32] M. J. Puska and R. M. Nieminen. "Atoms Embedded in an Electron Gas: Phase Shifts and Cross Sections". In: *Phys. Rev. B* 27 (1983), p. 6121. DOI: 10.1103/PhysRevB.27.6121.

[33] B. Hellsing and M. Persson. "Electronic Damping of Atomic and Molecular Vibrations at Metal Surfaces". In: *Phys Scr* 29 (1984), p. 360. DOI: 10.1088/0031-8949/29/4/014.

[34] M. Askerka, R. J. Maurer, V. S. Batista, and J. C. Tully. "Role of Tensorial Electronic Friction in Energy Transfer at Metal Surfaces". In: *Phys. Rev. Lett.* 116 (2016), p. 217601. DOI: 10.1103/PhysRevLett.116.217601.

[35] R. J. Maurer, M. Askerka, V. S. Batista, and J. C. Tully. "Ab Initio Tensorial Electronic Friction for Molecules on Metal Surfaces: Nonadiabatic Vibrational Relaxation". In: *Phys. Rev. B* 94 (2016), p. 115432. DOI: 10.1103/PhysRevB.94.115432.

[36] M. Askerka, R. J. Maurer, V. S. Batista, and J. C. Tully. "Erratum: Role of Tensorial Electronic Friction in Energy Transfer at Metal Surfaces [Phys. Rev. Lett. 116, 217601 (2016)]". In: *Phys. Rev. Lett.* 119 (2017), p. 069901. DOI: 10.1103/PhysRevLett.119.069901.

[37] M. S. Mizielinski, D. M. Bird, M. Persson, and S. Holloway. "Electronic Nonadiabatic Effects in the Adsorption of Hydrogen Atoms on Metals". In: *J. Chem. Phys.* 122 (2005), p. 084710. DOI: 10.1063/1.1854623.

[38] J. R. Trail, M. C. Graham, and D. M. Bird. "Electronic Damping of Molecular Motion at Metal Surfaces". In: *Computer Physics Communications* 137 (2001), pp. 163–173. DOI: 10.1016/S0010-4655(01)00177-1.

[39] J. R. Trail, M. C. Graham, and D. M. Bird. "Electronic Damping of Molecular Motion at Metal Surfaces". In: *Computer Physics Communications* 137 (2001), pp. 163–173. DOI: 10.1016/S0010-4655(01)00177-1.

[40] R. J. Maurer, B. Jiang, H. Guo, and J. C. Tully. "Mode Specific Electronic Friction in Dissociative Chemisorption on Metal Surfaces: H_2 on Ag(111)". In: *Phys. Rev. Lett.* 118 (2017), p. 256001. DOI: 10.1103/PhysRevLett.118.256001. arXiv: 1705.09753 [cond-mat.mtrl-sci].

[41] Y. Zhang, R. J. Maurer, H. Guo, and B. Jiang. "Hot-Electron Effects during Reactive Scattering of H_2 from Ag(111): The Interplay between Mode-Specific Electronic Friction and the Potential Energy Landscape". In: *Chem. Sci.* 10 (2019), pp. 1089–1097. DOI: 10.1039/C8SC03955K.

[42] R. J. Maurer, Y. Zhang, H. Guo, and B. Jiang. "Hot Electron Effects during Reactive Scattering of H_2 from Ag(111): Assessing the Sensitivity to Initial Conditions, Coupling Magnitude, and Electronic Temperature". In: *Faraday Discuss.* 214 (2019), pp. 105–121. DOI: 10.1039/C8FD00140E.

[43] P. Spiering and J. Meyer. "Testing Electronic Friction Models: Vibrational De-Excitation in Scattering of H_2 and D_2 from Cu(111)". In: *J. Phys. Chem. Lett.* 9 (2018), pp. 1803–1808. DOI: 10.1021/acs.jpclett.7b03182.

[44] P. Spiering, K. Shakouri, J. Behler, G.-J. Kroes, and J. Meyer. "Orbital-Dependent Electronic Friction Significantly Affects the Description of Reactive Scattering of N_2 from Ru(0001)". In: *J. Phys. Chem. Lett.* 10 (2019), pp. 2957–2962. DOI: 10.1021/acs.jpclett.9b00523.

[45] D. Novko, M. Alducin, and J. I. Juaristi. "Electron-Mediated Phonon-Phonon Coupling Drives the Vibrational Relaxation of CO on Cu(100)". In: *Phys. Rev. Lett.* 120 (2018), p. 156804. DOI: 10.1103/PhysRevLett.120.156804.

[46] Z. Jin and J. E. Subotnik. "A Practical Ansatz for Evaluating the Electronic Friction Tensor Accurately, Efficiently, and in a Nearly Black-Box Format". In: *J. Chem. Phys.* 150 (2019), p. 164105. DOI: 10.1063/1.5085683.